Journal of Alloys and Compounds 509S (2011) S621–S624

Contents lists available at ScienceDirect

Journal of Alloys and Compounds

journal homepage: www.elsevier.com/locate/jallcom

Correlation between hydrogen migration and microstructure in cast Mg alloys

Y.H. Cho*, A.K. Dahle

Materials Engineering, The University of Queensland, Frank White Bldg. #43, Brisbane, QLD 4072, Australia

ARTICLE INFO

Article history:
Received 17 July 2010
Received in revised form 12 October 2010
Accepted 22 October 2010
Available online 4 November 2010

Keywords:
Mg alloys
Hydrogen storage
Eutectic
Intermetallics
Porous structure

ABSTRACT

A simple casting process has been applied to produce binary Mg–X (X = Ni, Cu or Al) in situ composites for hydrogen storage. Besides a major single phase of primary Mg, nanostructured eutectic networks of Mg–Mg_2Ni, Mg–Mg_2Cu and Mg–$Mg_{17}Al_{15}$ were formed during solidification of Mg–Ni, Mg–Cu and Mg–Al alloys, respectively. Each intermetallic phase has different effects on the hydrogen sorption kinetics of the Mg alloys due to their different reactivities with hydrogen. In this study, the relationship between hydrogen migration and microstructure of the cast Mg alloys is investigated. The influence of hydrogenation/dehydrogenation cycling on the formation of porous structures is further discussed.

1. Introduction

Magnesium can reversibly store up to 7.6 wt.% hydrogen and has therefore been suggested to be one of the most promising hydrogen storage materials. However, in order to utilise magnesium for hydrogen storage the drawbacks of high thermodynamic stability of MgH_2 which leads to high desorption temperature (around 300 °C for 0.1 MPa hydrogen pressure) needs to be overcome. Earlier studies reported that alloying with Ni or Cu, which form Mg_2Ni and Mg_2Cu intermetallics, significantly decreases the temperature required for release of hydrogen [1–3]. Furthermore, various processing methods such as ball-milling Mg into nano-crystalline powder [4,5], mechanical alloying with transition metals [6,7] as well as oxides [8], and melt spinning [9] have been attempted to catalyse the dehydrogenation kinetics of the MgH_2 while maintaining a reasonable storage capacity.

Our recent work has shown that controlled solidification processing can be used to produce primary α-Mg and in situ composites of eutectic Mg–Mg_2Ni with an interlamellar spacing of a few hundred nanometers [10]. Given that the hydrogen sorption kinetics is strongly influenced by the catalytic phase, i.e. Mg_2Ni, producing a homogeneous and continuous mixture of the phase with a large interface area in the nanostructured Mg–Mg_2Ni eutectic is highly desirable. This can be accomplished by a melting and solidification technique. Besides the Mg–Ni system, binary Mg–Cu and Mg–Al alloys containing eutectic mixtures of Mg–Mg_2Cu and Mg–$Mg_{17}Al_{12}$ have also been studied as classic hydrogen storage materials [2,3,11,12]. However, the different intermetallic phases present in the eutectic networks of Mg alloyed with Ni, Cu and Al interacts with hydrogen differently and undergo either hydride formation [1] or disproportionation [2,11]. This influences the rate-limiting step of the dehydrogenation kinetics of the Mg alloys which has been analysed by fitting with well-defined kinetic models [13,14] and recently discussed by the authors [15].

In the present paper, we characterise the microstructural aspects of these materials to identify the sites and phases which hydrogen preferentially accesses and migrates through with high mobility. Furthermore, we discuss the differences in the reactivity of intermetallics with hydrogen and thus investigate its influence on reconstructing the morphology of the binary Mg–X (X = Ni, Cu and Al) alloys.

2. Experimental

Binary Mg–10 wt.% Ni, Mg–20 wt.% Cu and Mg–15 wt.% Al alloys with an average weight of 1 kg were melted in a steel crucible in an electric resistance furnace at 760 °C under cover gas ($CO_2 + SF_6$) atmosphere. Commercial purity magnesium (99.8%), nickel (99.8%), Cu (electrical grade) and Al (99.9%) were used for alloying. The melts were skimmed and cast into preheated cylindrical steel moulds (15 mm diameter, 200 mm height and 30 mm wall thickness). Hydrogen absorption and desorption rates were measured under pressures of 2 MPa and 0.1 MPa, respectively, and at a temperature of 350 °C in a Sieverts's apparatus designed by Suzuki Shokan Co. Ltd., Japan. 0.25 g of chip samples for hydrogen testing was prepared by drilling the cast ingots. Characterization of the microstructures and chemical composition of the constituent phases was carried out in a scanning electron microscope (SEM) with an energy dispersive X-ray spectrometer (EDS).

* Corresponding author.
E-mail address: y.cho@uq.edu.au (Y.H. Cho).

0925-8388/$ – see front matter © 2010 Elsevier B.V. All rights reserved.
doi:10.1016/j.jallcom.2010.10.123

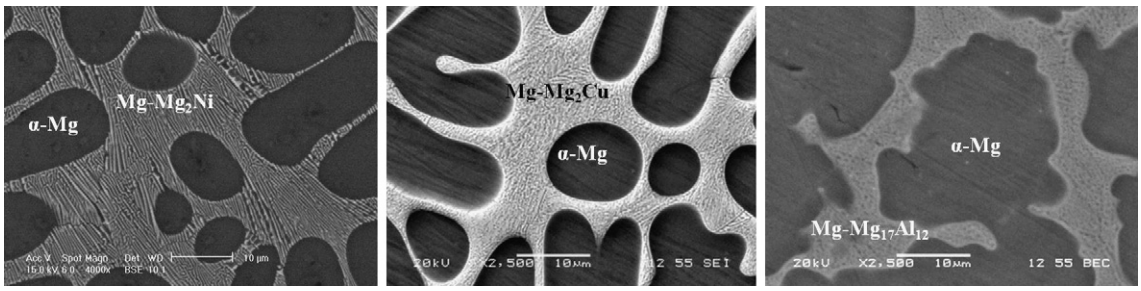

Fig. 1. SEM micrographs of the cast alloys showing primary α-Mg dendrites and (a) eutectic Mg–Mg_2Ni in Mg–10 wt.% Ni alloy; (b) eutectic Mg–Mg_2Cu in Mg–20 wt.% Cu alloy; and (c) Mg–$Mg_{17}Al_{12}$ in Mg–15 wt.% Al alloy.

3. Results and discussion

Fig. 1 shows SEM micrographs of the cast Mg alloys produced by controlled solidification, consisting of α-Mg matrix surrounded by a continuous network of eutectic with an interlamellar spacing on the order of a few hundred nanometers. The addition of Ni, Cu or Al to Mg forms Mg_2Ni, Mg_2Cu and $Mg_{17}Al_{12}$ intermetallics, respectively, which are present in the eutectic mixtures together with Mg phase.

Drilled chips from the cast ingots were used for hydrogen sorption testing. The dehydriding behaviour of the alloys was measured at 350 °C and 0.1 MPa and the results are shown in Fig. 2. In Fig. 2(a) the dehydrogenation fraction for the Mg–10 wt.% Ni alloy shows a sharp parabolic shape whereas typical S-shaped curves were observed for both Mg–20 wt.% Cu and Mg–15 wt.% Al alloys. Despite the large surface area introduced by drilling, the results suggest that the initiation of hydrogen release does not always occur on the surface, but rather rely on the reactive nature of the alloy (constituent phases and morphology) with hydrogen. As recently discussed [15], the intermetallics present in the eutectic such as Mg_2Ni, Mg_2Cu and $Mg_{17}Al_{12}$ play a crucial role in nucleating Mg from MgH_2 on dehydrogenation and therefore affect the dehydriding kinetics of each alloy differently.

Fig. 3(a) shows a backscattered electron (BSE) micrograph of the as-drilled Mg–10 wt.% Ni alloy where the eutectic network is clearly visible. After several hydrogenation/dehydrogenation cycles, a porous structure was observed in the eutectic Mg–Mg_2Ni region as shown in Fig. 3(b) while the original shape of the chip sample was retained. Cracks are also observed at the interface between primary α-Mg (dark grey) and the eutectic (light grey) (see Fig. 3(b)). It has been suggested that Mg_2Ni initiates hydrogen absorption [16,17] which then diffuses into the adjacent Mg and forms MgH_2 [12]. As shown in Fig. 2(a) and (b), the kinetic behaviour

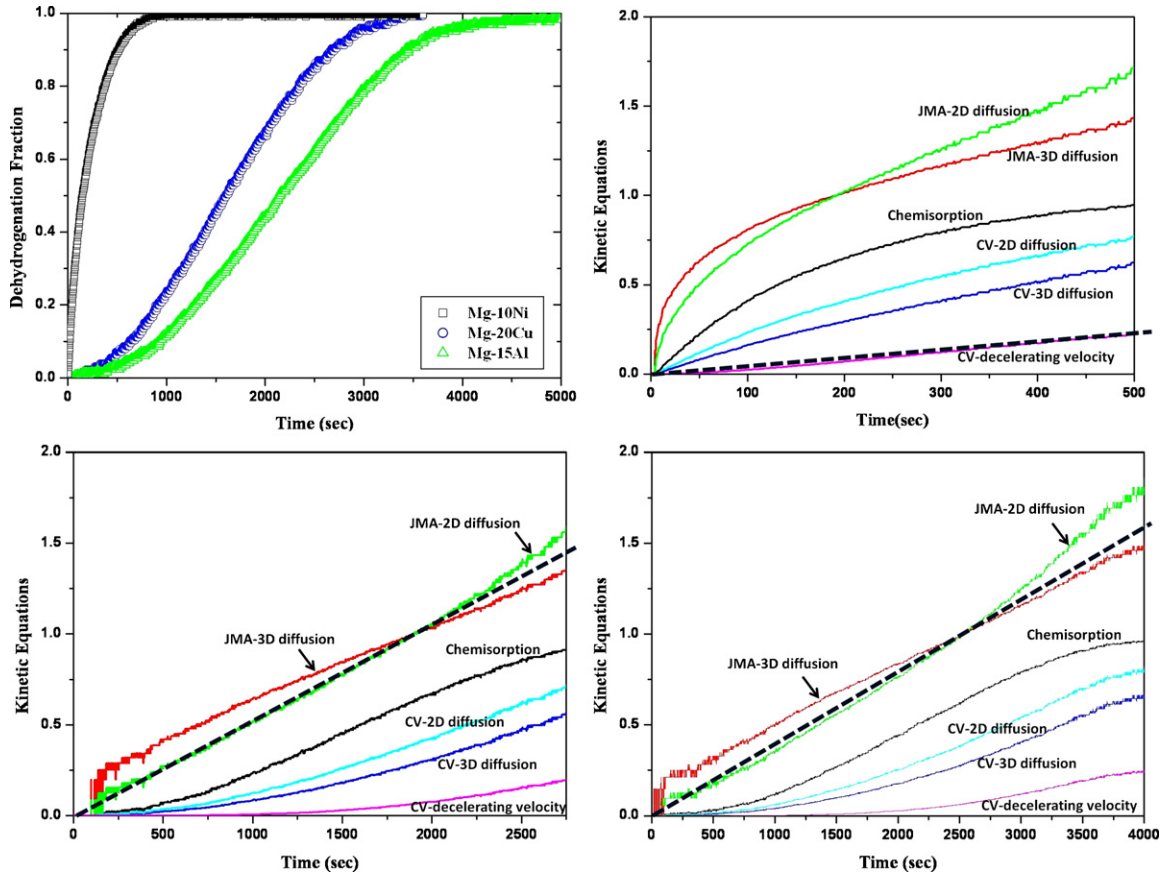

Fig. 2. (a) Dehydrogenation kinetics of the Mg alloys at 350 °C and 0.1 MPa. Results of fitting different kinetic models [13,14] to the experimental dehydrogenation results for (b) Mg–10 wt.% Ni, (c) Mg–20 wt.% Cu and (d) Mg–15 wt.% Al alloys.

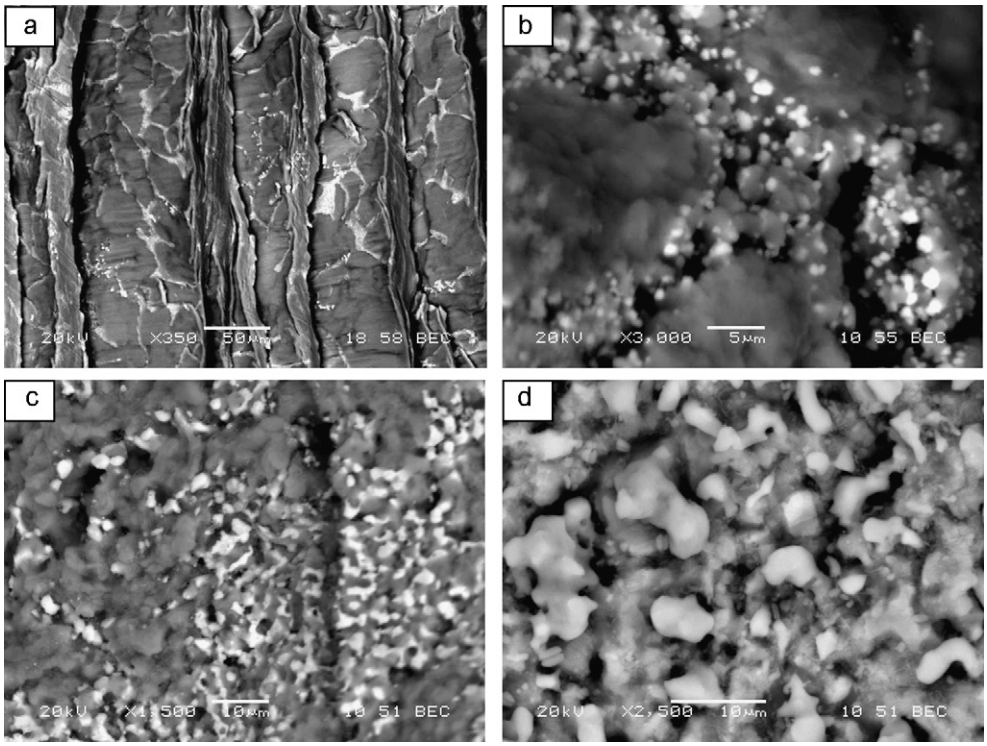

Fig. 3. BSE micrographs of chipped samples of (a) as-drilled Mg–10 wt.% Ni and hydrogen tested (b) Mg–10 wt.% Ni; (c) Mg–20 wt.% Cu; (d) Mg–15 wt.% Al chips.

of hydrogen desorption of the Mg–10 wt.% Ni alloy fits well with the contracting volume (CV) model with a decelerating interface velocity $(1-(2\alpha/3)-(1-\alpha)^{2/3}=kt)$ where α, k and t are dehydrogenation fraction, reaction constant and time respectively [14]. This indicates that Mg_2Ni, which has a certain range of hydrogen solubility, prompts the nucleation of Mg and thus nucleation itself is no longer rate-limiting. It is therefore considered that the preferential hydrogen migration through the eutectic Mg–Mg_2Ni network leads to a volumetric expansion of both Mg and Mg_2Ni, up to approximately 30% molar volume [18], in association with the formation of hydrides. This generates extensive stresses in the eutectic array and results in the localised formation of the porous structure in the interior of the eutectic and the creation of cracks in the Mg–10 wt.% Ni alloy. The EDS maps in Fig. 4 of the distribution of Mg and Ni indicate that the pore sites correspond to the location of the host metal, i.e. eutectic Mg phase. The colour bar on the left hand corner of Fig. 4(b) and (c) represents the intensity of Mg and Ni respectively and a red colour in the image indicates an intense signal of each element.

The Mg–Cu and Mg–Al chips, on the other hand, exhibit a more homogeneous distribution of pores which are observed throughout the samples after hydrogen cycling as shown in Fig. 3(c) and (d) respectively. Despite the very similar eutectic networks of Mg–Mg_2Cu and Mg–$Mg_{17}Al_{12}$ compared to Mg–Mg_2Ni, the tendency of hydrogen segregation towards the eutectic region in both Mg–20 wt.% Cu and Mg–15 wt.% Al alloys is not as significant as in the Mg–10 wt.% Ni alloy. This is probably due to the difference in reactivity of the intermetallics, i.e. Mg_2Cu and $Mg_{17}Al_{12}$, with hydrogen. Both Mg_2Cu and $Mg_{17}Al_{12}$ have been suggested to have oxide-free or less contaminated oxide layers on the surface through which hydrogen penetration is accelerated upon hydrogenation [3,19,20]. Instead of forming a ternary hydride phase, the catalytic role of the intermetallics is more likely related to the disproportionation when decomposing into MgH_2 and intermetallic products such as $MgCu_2$ [2,3] and Mg_2Al_3 [11] when reacting with high pressure hydrogen. This may result in the reconstruction and fragmentation of the eutectic Mg–Mg_2Cu and Mg–$Mg_{17}Al_{12}$ with spalling of a brittle metal hydride phase.

As shown in Fig. 2(c) and (d), the dehydrogenation results for both Mg–20 wt.% Cu and Mg–15 wt.% Al alloys display the best fit with a random nucleation and growth model, i.e. the Johnson–Mehl–Avrami (JMA) model with an exponent $n=2$ $(1-\alpha=\exp[-(kt)^n]$, where α, k, t, n are dehydrogenation fraction,

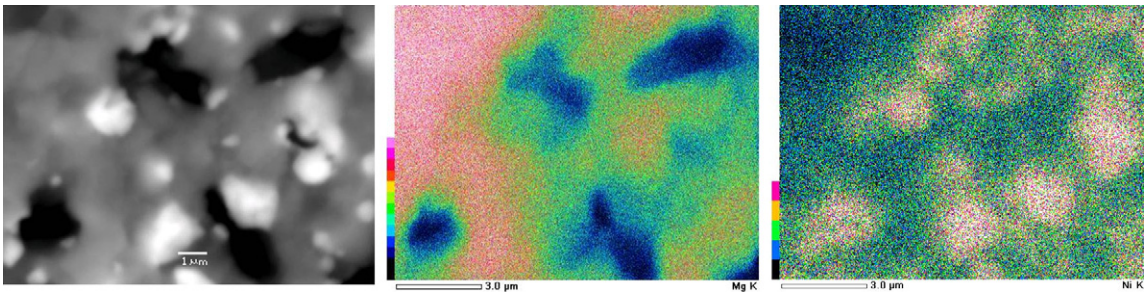

Fig. 4. (a) BSE micrograph showing the porous structure in the interior of eutectic Mg–Mg_2Ni in Mg–10 wt.% Ni alloy after hydrogen testing. EDS maps showing the distributions of (b) Mg and (c) Ni. The intensity of each element is visualised by the colour bar where a red colour indicates an intense signal.

reaction constant, time and the order of dimension respectively) [13]. This is likely caused by the fact that Mg_2Cu and $Mg_{17}Al_{12}$, which have no solubility of hydrogen, are less effective in catalysing the nucleation of Mg from MgH_2 compared to Mg_2Ni. Hence the nucleation and growth of Mg from MgH_2 in the alloys is diffusion controlled and occurs randomly throughout the sample. It is also suggested that hydrogen atoms can most efficiently diffuse along the eutectic interphase boundaries and thus quickly reach both α-Mg and the eutectic region. Consequently, the hydrogen migration in the Mg–20 wt.% Cu and Mg–15 wt.% Al alloys is rather homogeneous and less stress development is expected in the eutectic networks compared to eutectic Mg–Mg_2Ni.

4. Conclusions

Hydrogenation/dehydrogenation cycling of cast Mg–10 wt.% Ni, Mg–20 wt.% Cu and Mg–15 wt.% alloys leads to reconstructing the as-cast microstructures with the formation of characteristic porous structures. Localised pores forming in the interior of eutectic Mg–Mg_2Ni are observed in the Mg–10 wt.% Ni alloy, whereas the distribution of pores is rather homogeneous in Mg–20 wt.% Cu and Mg–15 wt.% Al alloys. This suggests that the reactivity of the intermetallics in the eutectic networks of Mg–Mg_2Ni, Mg–Mg_2Cu and Mg–$Mg_{17}Al_{12}$ with hydrogen is critical for hydrogen migration and controls the overall hydrogen sorption kinetics of the Mg alloy. Stress development in the eutectic networks as well as the brittle host metal hydride, MgH_2, during high pressure hydrogen penetration are proposed to play a key role for pore formation in the Mg alloys.

Acknowledgements

The authors gratefully acknowledge funding form the National Hydrogen Metal Alliance (NHMA) supported by the CSIRO Energy Transformed Flagship and the ARC Discovery Project, DP087715.

References

[1] J.J. Reilly, R.H. Wiswall, Inorg. Chem. 7 (1968) 2254.
[2] J.J. Reilly, R.H. Wiswall, Inorg. Chem. 6 (1967) 2220.
[3] A. Karty, J. Grunzweiggenossar, P.S. Rudman, J. Appl. Phys. 50 (1979) 7200.
[4] S. Orimo, H. Fujii, K. Ikeda, Acta Mater. 45 (1997) 331.
[5] A. Zaluska, L. Zaluski, J.O. Strom-Olsen, J. Alloys Compd. 288 (1999) 217.
[6] A. Zaluska, L. Zaluski, J.O. Strom-Olsen, J. Alloys Compd. 289 (1999) 197.
[7] G. Liang, J. Huot, S. Boily, A. Van Neste, R. Schulz, J. Alloys Compd. 292 (1999) 247.
[8] G. Barkhordarian, T. Klassen, R. Bormann, J. Phys. Chem. B 110 (2006) 11020.
[9] C.D. Yim, B.S. You, Y.S. Na, J.S. Bae, Catal. Today 120 (2007) 276.
[10] Y. Cho, A.K. Dahle, Mater. Sci. Forum 638–642 (2010) 1085.
[11] A. Andreasen, Int. J. Hydrogen Energy 33 (2008) 7489.
[12] D.L. Douglass, Metall. Trans. A 6 (1975) 2179.
[13] M.H. Mintz, J. Bloch, Prog. Solid State Chem. 16 (1985) 163.
[14] M.H. Mintz, Y. Zeiri, J. Alloys Compd. 216 (1995) 159.
[15] Y.H. Cho, A.K. Dahle, Mater. Sci. Forum 654–656 (2010) 2863.
[16] A. Seiler, L. Schlapbach, T. Vonwaldkirch, D. Shaltiel, F. Stucki, J. Less-Common Met. 73 (1980) 193.
[17] L. Schlapbach, A. Seiler, F. Stucki, H.C. Siegmann, J. Less-Common Met. 73 (1980) 145.
[18] S. Ono, Y. Ishido, K. Imanari, T. Tabata, Y.K. Cho, R. Yamamoto, M. Doyama, J. Less-Common Met. 88 (1982) 57.
[19] A. Andreasen, M.B. Sorensen, R. Burkarl, B. Moller, A.M. Molenbroek, A.S. Pedersen, J.W. Andreasen, M.M. Nielsen, T.R. Jensen, J. Alloys Compd. 404 (2005) 323.
[20] A. Andreasen, M.B. Sorensen, R. Burkarl, B. Moller, A.M. Molenbroek, A.S. Pedersen, T. Vegge, T.R. Jensen, Appl. Phys. A 82 (2006) 515.